POS-A-11

Experimental Verification for ESPAR Antenna to Suppress Interference in 2.4-GHz Band Wireless LAN Transmission

Atsushi Honda[†], Takeshi Toda[†], Yuuta Nakaya[†], Kaoru Yokoo[†], Jun-ichi Takada[‡], and Yasuyuki[†] Oishi

[†] Fujitsu, Ltd. 5-5 Hikari-no-oka Yokosuka 239-0847 Japan,

[‡] Tokyo Institute of Technology, 2-12-1 Oh-okayama Meguro Tokyo 152-8552 Japan,

[†] ahonda@labs.fujitsu.com, [‡] takada@ide.titech.ac.jp

1. Introduction

Various wireless communication technologies have recently appeared for personal networks and they are causing overcrowding on the limited frequency resources for personal wireless communication. There is even a trend to share frequency resources without licenses as "Commons." However, different communication systems interfere with each other in the same frequency bands or channels. For example, in the 2.4-GHz ISM band, microwave ovens and Bluetooth interfere with wireless LAN standard IEEE802.11b/g [1]. In the 5.2-GHz band, ultra wideband (UWB: 3.1-10.6 GHz) is assumed to interfere with IEEE802.11a [2]. It is impossible to design an interference-free system by standardization, because new technologies quickly emerge. Moreover, intersymbol interference (ISI) and co-channel interference have increased because of the recent coverage-expansion and rapid growth in the number of subscribers in urban areas. Furthermore, many illegal radio waves may emerge as software defined radio techniques become popular [3]. Thus, for user terminals, it has become much more important to suppress such kinds of interference at reception and to avoid interfering with other stations at transmission. Interference-tolerant technologies thus facilitate high-data-rate and high-quality transmission.

The adaptive array antenna (AAA) is one of the most promising techniques for overcoming interference without any pre-knowledge of the signal nature, direction of arrival (DOA), or time delay of arrival [4]. AAAs are classified into two types: digital and analogue processing types. Digital ones need as many RF (radio frequency) front-ends and A/D converters as antenna branches, so it is difficult to use them for terminals in terms of power consumption, size, and cost. Analogue ones have array processing in the RF part, so they are suitable for terminals [5]. The RF-AAAs have already been developed for satellite communications, military radars, and aerospace applications [5]-[7]. However, there has recently been a shift in its use towards personal communications [5], [8]-[10]. For example, an RF-AAA has been proposed for mitigating the ISI in high-speed wireless LANs (WLANs) [8], and another RF-AAA has been put to commercial use in WLAN access points for beam-forming towards terminals [9]. Furthermore, recent advances in monolithic microwave integrated circuits and micro-electromechanical system technologies for variable-gain low-noise amplifiers and phase shifters have facilitated the implementation of RF-AAA into terminals [11][12].

Electronically steerable passive array radiator (ESPAR) antenna was recently put into practical use as an analogue adaptive array antenna for ad-hoc terminals by Dr. Ohira's research group in Japan [5], after being originally investigated for military radar in the US [6], [7]. The ESPAR antenna is aerial beamformer using space-coupled parasites with varactor termination. Its beam-steering effect has been demonstrated for ad-hoc networking [13] and its null-steering effect for suppressing interference has been investigated by computer simulations [14], [15], but it has not yet been demonstrated to the best of our knowledge.

This paper demonstrates null-steering of the ESPAR antenna to suppress interference for wireless LAN (WLAN) system in the 2.4-GHz band. The WLAN standards IEEE802.11g and IEEE802.11b are used for transmission and interference signals respectively. Steepest gradient algorithm is used to adjust varactors in the ESPAR antenna [16]. The effect of the null-forming is quantified using the three-dimensional (3-D) directional pattern and bit error rate (BER) measurement. The results show that the ESPAR antenna forms a deep null with respect to the interference and thus significantly improves the BER performance.

2. Experimental System

Figure 1 shows a block diagram of the experimental system, which consists of two transmitters, an RF-AAA, a receiver, and digital signal processing (DSP) systems on a PC, and a bias supply for controlling variable devices in the RF-AAA.

2.1 Transmitters

Two signal generators (Agilent E4438C) are employed as transmitters. One is for the desired signal and the other acts as an interference source. Commercially available sleeve dipole antennas are used for both transmitter antennas.

2.2 Receiver

In the receiver (VSA 89641A), RF-AAA output signal is down-converted to an intermediate frequency (IF) signal and gain-controlled to an appropriate level with a gain-controlled amplifier. The gain-controlled IF signal is quasi-coherently detected by a quadrature demodulator. The quasi-coherently detected signal is passed through root roll-off filters and digitized by an A/D converter. The receiver finally outputs digital data bursts into the PC through IEEE 1394 cable according to a trigger signal for data acquisition. Carrier and frame synchronizations are hard-wired.

2.3 DSP systems on PC

BER for the data bursts from the receiver is measured by Agilent Ptolemy simulator on the PC. Agilent VEE Pro executes an adaptive control algorithm for the RF-AAA using a long preamble part of the received data burst and controls the bias supply through GP-IB. By using this experimental system, we can test various types of RF-AAA. Real-time online processing is required for the RF-AAA unlike offline processing for DSP-type AAAs, because the receiver receives only one output signal after RF-AAA processing and adaptive control is required in real time through bursts stream.

Fig. 1 Experimental system.
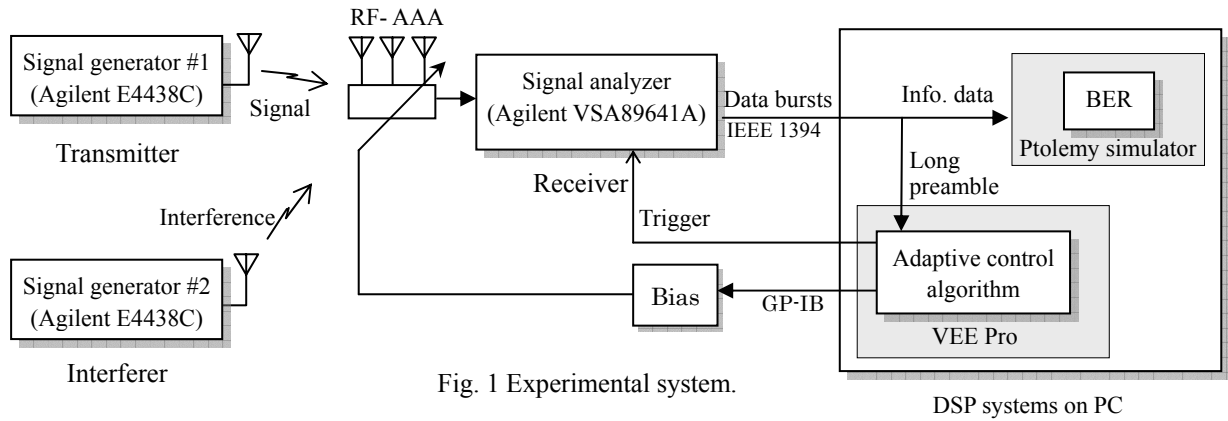
2.4 Control criterion and timing chart

We use steepest gradient algorithm to control the RF-AAA, in which a cost function is calculated according to the cross-correlation coefficient, which is expressed as [16]:
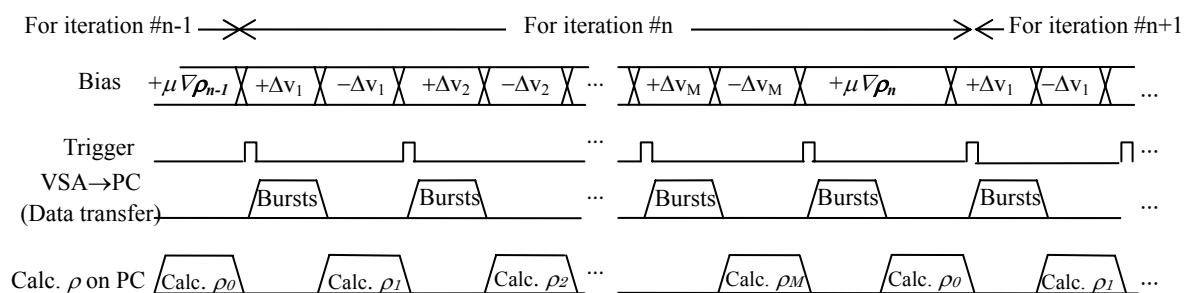
$$\rho_n = y^H(n)r(n) \Big/ \left(\sqrt{y^H(n)y(n)} \sqrt{r^H(n)\,r(n)} \right)$$

where y(n) and r(n) are a long preamble pattern of the received signal and a reference signal, respectively, at time n. **Figure 2** shows the timing chart of data flow, bias, acquisition trigger, and the calculation of the cost function in the adaptive control. The bias voltage for the m-th variable device is perturbed ($+\Delta v_m$) and the correlation coefficients (ρ_m) are calculated for all variable devices in each iteration. Varctor number m corresponds to parasitic elements number ($m = 1, 2, \cdots, M$). Then, the bias vector is updated using a gradient vector of the correlation coefficients $\nabla\rho_n$ and a step size parameter μ as follows.

$$\mathbf{v}(n+1) = \mathbf{v}(n) + \mu\nabla\mathbf{\rho}_n$$

2.5 BER measurement

The experiment system measures BER by comparing receive and reference data bursts in Agilent ADS Ptolemy simulator implemented on the PC. The Ptolemy simulator measures the BER for each block of bursts obtained from the receiver with the acquisition trigger, shown in **Fig. 2**. Option 002 (32M samples) for the transmitter (SG E4438C) allows the experimental system to measure BER accurately. Here, for 18-Mbps QPSK, the maximum number of transmitted bursts is 847 when the over-sampling rate is four and the amount of data per burst is 1000 bytes. Then, 6,776,000 bits (= 1000 bytes × 8 bits × 847 bursts) is the maximum number of transmitted bits, and that is more than enough to measure BER reliably on the order of 10^{-4}.

For iteration #n-1 ⟶ ⟶ For iteration #n ⟶ ⟶ For iteration #n+1

Bias: $+\mu\overline{\nabla\rho_{n-1}}$ $+\Delta v_1$ $-\Delta v_1$ $+\Delta v_2$ $-\Delta v_2$ ... $+\Delta v_M$ $-\Delta v_M$ $+\mu\overline{\nabla\rho_n}$ $+\Delta v_1$ $-\Delta v_1$ ...

Trigger ...

VSA→PC (Data transfer): Bursts Bursts ... Bursts Bursts Bursts ...

Calc. ρ on PC: Calc. ρ_0 Calc. ρ_1 Calc. ρ_2 ... Calc. ρ_M Calc. ρ_0 Calc. ρ_1 ...

Fig. 2 Timing chart of data flow, bias, acquisition trigger, and calculation of cost function.

3. Experiment

Table 2 lists parameters for the experiment. **Figure 3** shows a manufactured ESPAR antenna in which a feeding port is located in center and surrounded by six parasitic elements (M=6) with varactor termination.

3.1 Experimental parameters

The transmitted signal is IEEE802.11g with 18-Mbps QPSK and the interference signal is IEEE802.11b with 11-Mbps CCK. The signal-to-interference ratio (SIR) was set to 0dB at 99.9% of the bandwidth of the transmitted signal. The experiment was carried out in an anechoic chamber and only downlink transmission was tested. The transmitting and receiving antennas were placed at equal heights. The DOAs of the transmitted signal and interference were 0° and 120°, respectively.

Table 2   Experimental Parameters

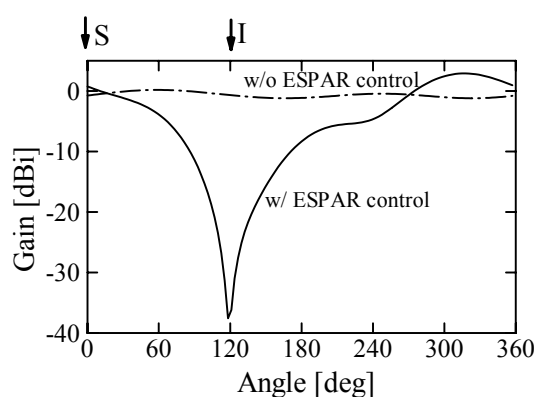| Receive antenna	ESPAR antenna
Frequency	2.484GHz
Signal	IEEE802.11g, 18-Mbps QPSK
Interference	IEEE802.11b, 11-Mbps CCK
DOA	Signal: φ=0° Interference: φ=120°
Input SIR	0 dB (@99.9% of bandwidth)
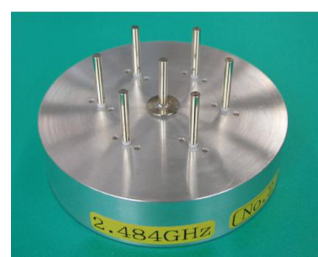
Fig. 3 ESPAR antenna.

3.2 Array directional pattern

Figures 4 and **5** show array directional patterns measured in 3-D and in the horizontal plane (X-Y plane in Fig. 4) respectively, after convergence of the adaptive control. A deep null was observed in the direction of interference, φ=120°. Antenna gain was +0.7 dBi in the direction of the desired signal (φ=0°) and −36 dBi in the direction of the interference (at φ=120°), so the output SIR was 36.7 dB. The result without bias also shown in **Fig. 5** is nearly omni-directional and its gain is −0.7dBi in the direction of the desired signal (φ=0°). Therefore, the gain in the direction of the desired signal was 1.4 dB higher after adaptive control. The gain (+0.7 dBi) of the ESPAR antenna in the direction of the desired signal (φ=0°) was not maximum because of some antenna configuration impairment etc.
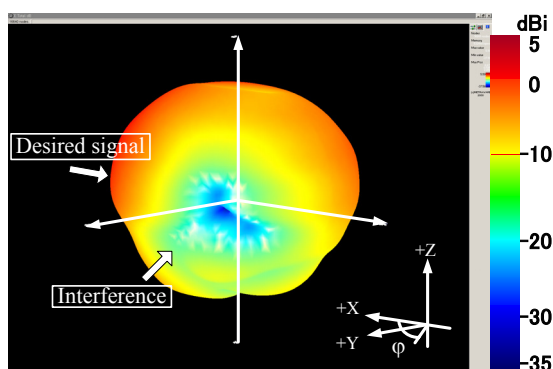
Fig.4 Array directional pattern in 3-D.

Fig. 5 Array directional pattern in X-Y plane.

3.3 BER performance

Figure 6 shows BER performance for the ESPAR antenna with and without the interference. To evaluate the effect of the ESPAR antenna without including the receiver unit, we measured the BER while varying the output power of the transmitter. First, the BER was measured without the interference. The BER result without control showed a similar tendency to that obtained by theoretical calculation assuming a 2.14-dBi standard antenna. This confirmed that the experimental system was working correctly. Degradation of the BER compared to the theory is mainly due to the antenna gain in the direction of the desired signal (i.e., $0.7 - 2.14 = -1.44$ dB). Second, BER was measured with the interference. Without control, the BER was 0.5. With control, it was significantly improved and was almost the same as that without interference.
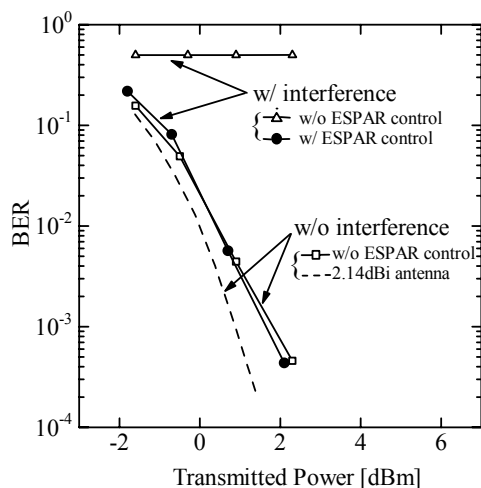

Fig. 6 BER performance.

4. Conclusion

We developed an adaptive control system for RF adaptive array antennas and a BER measurement system in WLAN transmission. We manufactured an ESPAR antenna for the 2.4-GHz band. The transmitting signal was IEEE802.11g and the interference signal was IEEE802.11b. The measured array directional pattern showed that the ESPAR antenna output SIR was improved by about 37 dB by null-forming when input SIR was set to 0 dB. Consequently, the transmitted bits error performance was significantly improved and almost agreed with the case without interference.

Acknowledgments

References

[1] C-F Chiasserini and R. R. Rao, "Coexistence Mechanisms for Interference Mitigation in the 2.4-GHz ISM Band," Proc. 2003 IEEE Conf. on Ultra Wideband Systems and Technologies, Reston, VA, Nov. 17-19, 2003.

[2] A. Tomoki, T. Ogawa, and T. Kobayashi, "Experimental Evaluation of Interference from UWB ources to a 5-GHz Narrowband Digital Wireless Transmission System," Proc. 2003 IEEE Conf. on Ultra Wideband Systems and Technologies, Reston, VA, Nov. 17-19, 2003.

[3] J. Mitola, *Software Radio Architecture*, John Wiley & Sons, New York, 2000.

[4] R. A. Monzingo and T. W. Miller, *Introduction to Adaptive Arrays*, John Wiley & Sons, New York, 1980.

[5] T. Ohira, "Analog Smart Antennas: An Overview," Proc. The 13th IEEE Int'l Symp. On Personal, Indoor and Mobile Radio Communs., 2002 (PIMRC'02), Lisbon, Portogal, Sept. 2002.

[6] R. F. Harrington, "Reactively Controlled Directive Arrays," IEEE Trans. on AP., Vol. AP-26, No. 3, May 1978.

[7] R. J. Dinger, "A Planar Version of a 4.0 GHz Reactively Steered Adaptive Array," IEEE Trans. on AP., Vol. AP-34, No. 3, Murch 1986.

[8] A. Wittneben and U. Dersch, "On the potential of adaptive antenna combining for intersymbol interference reduction in high speed wireless LANs," IEEE Veh. Tech. Conf. (VTC), vol. 2, pp. 627-631, May 1997.

[9] Vivato Inc., "VivatoWi-Fi Systems Brochure," Mar. 2003.

[10] F. Ellinger and W. Bachtold, "Adaptive antenna receiver module for WLAN at C-band with low power consumption," IEEE Trans. on MTTs, vol. 51, no. 4, Apr. 2003.

[11] D. V. Thiel and S. Smith, *Switched Parasitic Antennas for Cellular Communications*, Artech House, Boston, 2002.

[12] H. J. De Los Santos, *RF MEMS Circuit Design for Wireless Coummunications*, Artech House, Boston, 2002.

[13] J. Cheng, M. Hashiguchi, K. Iigusa, and T. Ohira, "Electronically steerable parasitic array radiator antenna for omni- and sector pattern forming applications to wireless ad hoc networks, " IEE Proc.-Microw. Antennas Propag. vol.150, no.4, pp.203-208, Aug. 2003.

[14] T. Ohira, and K. Gyoda, "Electronically steerable passive array radiator antennas for low-cost analog adaptive beamforming, " 2000 IEEE Inter. Conf. on Phased array Systems & Technology, pp.101-104, Dana Point, California, 21-25, May 2000.

[15] A. Hirata, and T. Ohira, "Spotted null forming of electrically steerable parasitic array radiator antennas in indoor multipath propagation, " Asia-Pacific Microwave Conf., pp.189-191, Kyoto, Nov. 2002.

[16] J.Cheng, Y.Kamiya, and T.Ohira, "Adaptive beamforming of ESPAR antenna based on steepest gradient algorithm," IEICE Trans. Commun., vol.E84-B, no.7, pp.1790-1800, July 2001.